Aquatic Sciences (2019) 81:46
https://doi.org/10.1007/s00027-019-0644-1

Aquatic Sciences

RESEARCH ARTICLE

Observations and modeling of the surface seiches of Lake Tahoe, USA

Derek C. Roberts[1,2] · Heather M. Sprague[1,2,3] · Alexander L. Forrest[1,2] · Andrew T. Sornborger[4] · S. Geoffrey Schladow[1,2]

Received: 24 October 2018 / Accepted: 13 April 2019

Abstract

A rich array of spatially complex surface seiche modes exists in lakes. While the amplitude of these oscillations is often small, knowledge of their spatio-temporal characteristics is valuable for understanding when they might be of localized hydrodynamic importance. The expression and impact of these basin-scale barotropic oscillations in Lake Tahoe are evaluated using a finite-element numerical model and a distributed network of ten high-frequency nearshore monitoring stations. Model-predicted nodal distributions and periodicities are confirmed using the presence/absence of spectral power in measured pressure signals, and using coherence/phasing analysis of pressure signals from stations on common and opposing antinodes. Surface seiches in Lake Tahoe have complex nodal distributions despite the relative simplicity of the basin morphometry. Seiche amplitudes are magnified on shallow shelves, where they occasionally exceed 5 cm; elsewhere, amplitudes rarely exceed 1 cm. There is generally little coherence between surface seiching and littoral water quality. However, pressure–temperature coherence at shelf sites suggests potential seiche-driven pumping. Main-basin seiche signals are present in attached marinas, wetlands, and bays, implying reversing flows between the lake and these water bodies. On the shallow sill connecting Emerald Bay to Lake Tahoe, the fundamental main-basin seiche combines with a zeroth-mode harbor seiche to dominate the cross-sill flow signal, and to drive associated temperature fluctuations. Results highlight the importance of a thorough descriptive understanding of the resonant barotropic oscillations in any lake basin in a variety of research and management contexts, even when the magnitude of these oscillations tends to be small.

Keywords Surface seiche · Littoral · Lake Tahoe · Spectral analysis · Physical limnology

Introduction

Surface seiches are ubiquitous in enclosed and semi-enclosed water bodies (Korgen 1995). The spatial patterns and periods of these basin-scale barotropic standing waves are a function of basin geometry, water depth, and associated oscillatory resonance (Wilson 1972). The magnitude and persistence of their expression is driven by the balance between external excitation (often abrupt pressure fronts or wind gusts) and damping forces (bottom friction and, in the case of semi-enclosed basins, radiation through the open boundary).

Descriptive records of surface seiching in lakes date back centuries. Hollan et al. (1980) offer an English translation of observations of surface seiching on Lake Constance from 1549, and Forel (1893) famously described the surface oscillations of Lake Geneva in the nineteenth century. However, surface seiches received the most focused research attention in the 1970s and 1980s as spectral techniques and

✉ Derek C. Roberts
dcroberts@ucdavis.edu

Heather M. Sprague
heather.sprague@arcadis.com

Alexander L. Forrest
alforrest@ucdavis.edu

Andrew T. Sornborger
sornborger@lanl.gov

S. Geoffrey Schladow
gschladow@ucdavis.edu

1 Department of Civil and Environmental Engineering, University of California, Davis, CA, USA

2 UC Davis Tahoe Environmental Research Center, Incline Village, NV, USA

3 Arcadis US, Inc., San Francisco, CA, USA

4 Los Alamos National Laboratory, Los Alamos, NM, USA

Published online: 16 April 2019

two-dimensional numerical modeling emerged as practical tools for examining this physical phenomenon. Mortimer and Fee (1976) performed some of the pioneering work applying spectral analysis to lake level data to identify periods of lake surface oscillations in Lakes Michigan and Superior. In that same year, Rao and Schwab (1976) presented one of the first applications of a numerical eigenvalue scheme to the shallow-water equations to estimate the spatial distribution and periods of unique seiche modes in basins of arbitrary geometry. This approach, tested on Lakes Ontario and Superior, presented a major advance from Merian's formula (see Eq. 9.6 in Rabinovich 2009), which simplifies basin geometry to simple length and depths scales, and offers little insight into the spatial patterns of surface seiche expression. Rao et al. (1976) combined these techniques in a detailed analysis of Lake Michigan and adjoining Green Bay, presenting perhaps the standard approach for the majority of the surface seiche investigations that followed.

Schwab and Rao (1977) adopted the approach of Rao et al. (1976) to explore theoretical and observed seiche patterns in Lake Huron and, more specifically, to identify how main-basin oscillations are affected by, and drive oscillations in, adjoining bays. They confirmed the presence of zeroth-mode (also known as a Helmholtz, bay, or harbor mode; see Rabinovich 2009 for a detailed review) oscillations in each of the semi-enclosed bays, and showed how these combined-basin oscillations, unresolved in models of individual basins in isolation, can be important drivers of inter-basin exchange. Zeroth mode oscillations have nodes near the entrances to the attached water bodies, and peak amplitudes toward their far ends. Though the zeroth mode can be thought of as a co-basin mode, with resonant surface oscillations in adjoining basins driving currents in the narrows that connect them (Saylor and Sloss 1976; Saylor and Miller 1987), oscillations in the main basin can be imperceptibly weak when the attached bay is small relative to the main lake basin. This mode is theoretically present in all semi-enclosed water bodies. However, its excitation is dependent on the resonance of incoming long-wave oscillations from the main-basin; this concept has been likened to the tone generated by blowing the top of an empty glass bottle.

Following the application of these methodological advances to a handful of additional scenarios (i.e. Hollan et al. 1980; Hamblin 1982; Hutter et al. 1982), research on the topic in lakes became notably sparse. Okamoto and Endoh (1995) noted surface seiching as a relevant component of exchange between Lake Biwa and adjoining Shiozu Bay. In a review paper on exchange flows in lakes, Hamblin (1998) notes the importance of barotropic oscillations to harbor flushing. However, only a few recent hydrodynamic studies of lakes directly examine barotropic seiches. Rueda and Schladow's (2002) analysis of the basin-scale surface oscillations of Clear Lake was motivated by a need to explain a periodically reversing velocity signal measured in the inter-basin channel. However, the results of their study, linking model-predicted and observed seiche patterns to inter-basin flows, were never extended to a broader understanding of Clear Lake as a complete freshwater system. Kirillin et al. (2015) offer an analysis of the barotropic oscillations and associated currents in Flathead Lake (MT, USA), where seiche magnitudes regularly exceed 15 cm. However, their model-focused study did not directly investigate the impact of surface seiching on water quality or ecosystem processes. The review by Rabinovich (2009) references some of the seminal limnological work described above but refers almost exclusively to the oceanographic literature in describing more recent research. Similarly, Korgen's (1995) summary of the state of seiche-related research primarily references historical Laurentian Great Lakes studies.

A holistic understanding of littoral hydrodynamics is needed to fully understand complex nearshore ecosystem dynamics (Janssen et al. 2005). Though typically weaker than wind-wave or internal wave forcing, surface seiches may be relevant hydrodynamic features, particularly on shelves and sills at the lake periphery, and particularly during calm and/or unstratified periods when other hydrodynamic forces are weak or absent. The aim of this study is to detail surface seiche expression in a well-studied lake where this process is not generally considered, and, by relating results to lake management concerns, emphasize the potential relevance of surface seiches to lentic systems, even when their amplitudes are small.

We employ a finite-element numerical model and a distributed network of high-frequency nearshore monitoring stations (NS) to evaluate the expression and impact of surface seiches in deep, monomictic Lake Tahoe. Analysis of additional high-frequency pressure data, collected in a marina, a wetland, and a narrowly-connected bay, offers insight into seiche-driven exchange flow at the lake periphery. The latter analysis is supplemented by historical flow measurements from the mouth of the bay. Though qualitatively observable surface seiches are not a distinct feature of Lake Tahoe, there is evidence that a massive landslide triggered basin-shaping seiching several thousand years ago (Moore et al. 2006, 2014).

Surface seiches are a long-recognized phenomenon in lake basins. However, few analyses extend beyond a basic description of their expression. The combination of a comparatively fine-scale model grid and a spatially distributed network of high-frequency littoral water quality stations allows for a uniquely detailed characterization of the anatomy and impact of these oscillations in deep Lake Tahoe.

Methods

The development of a distributed network of high-frequency nearshore monitoring stations at Lake Tahoe (USA) has generated an ideal dataset for exploring processes with signals that vary in both time and space, such as surface seiches. Lake Tahoe (39°N, 120°W) is a deep (average depth ~ 300 m; maximum depth ~ 500 m), oligotrophic lake in the Sierra Nevada Mountains, USA (Fig. 1a). Thermal stratification typically persists from May through January. The lake annually mixes to several hundred meters, but only mixes the complete water column in especially cold winters (about every 3–7 years). With the exception of Emerald Bay, protruding from the lake's southwest corner (Fig. 1c), and shelves near Tahoe City, Tahoe Vista, and Timber Cove (TC, TV, and TB in Fig. 1a), the lake has relatively simple single-basin bathymetry.

Field data

Ten high-frequency nearshore monitoring stations (NS) are installed along the 2-m isobath at the perimeter of Lake Tahoe (Fig. 1a). Each station consists of an RBR Maestro conductivity–temperature–depth (CTD) unit coupled to a Turner Designs C3 fluorometer (C3) mounted to a weighted frame on the lakebed (sensors about 15 cm above

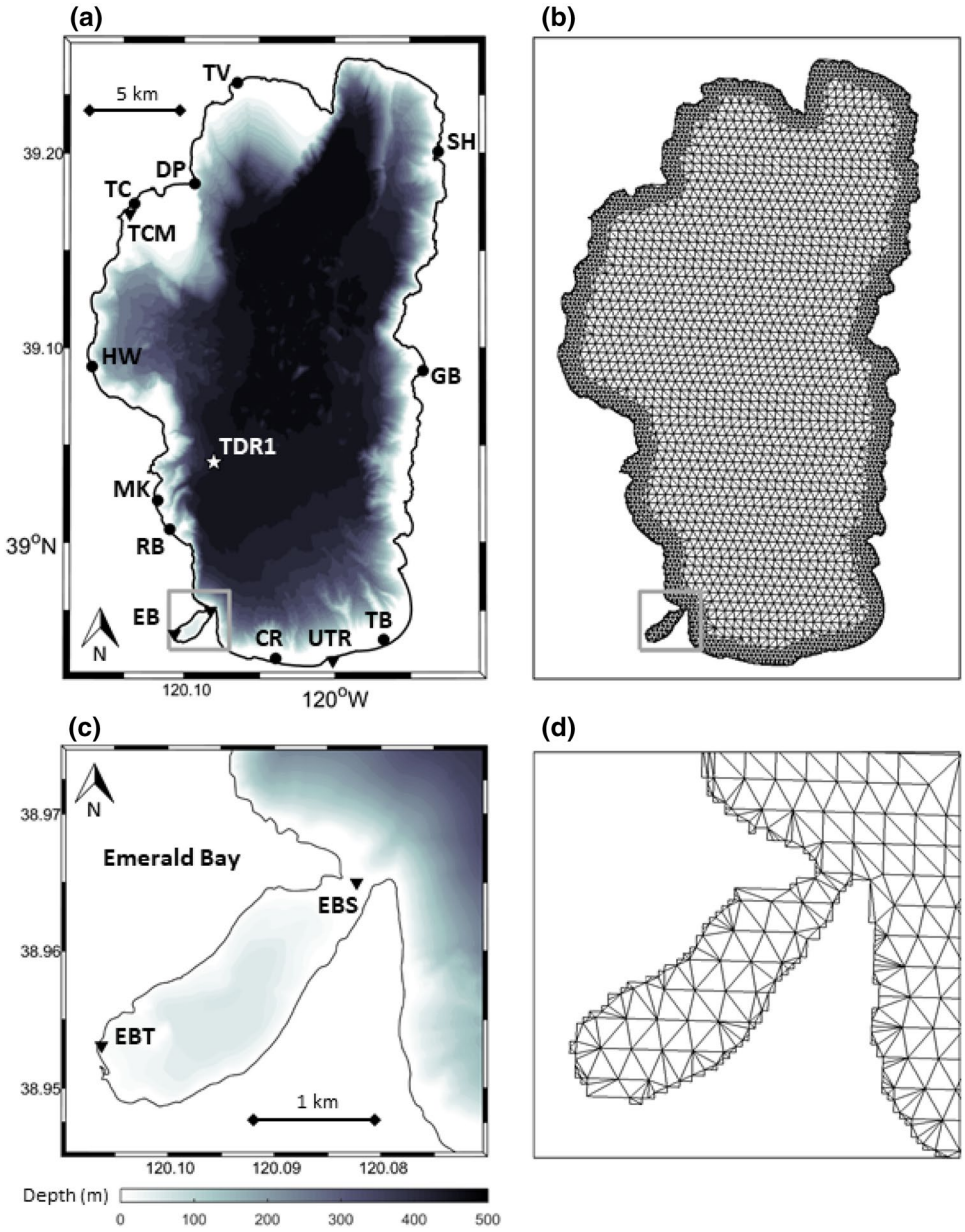

Fig. 1 **a** Lake Tahoe bathymetry. Circles show locations of nearshore stations: *RB* Rubicon, *MK* Meeks, *HW* Homewood; *TC* Tahoe City, *DP* Dollar Point, *TV* Tahoe Vista, *SH* Sand Harbor, *GB* Glenbrook, *TB* Timber Cove, *CR* Camp Richardson. Triangles show locations of supplemental temperature-depth sensor deployments: *TCM* Tahoe City Marina, *UTR* Upper Truckee River wetland, *EB* Emerald Bay. Star shows the location of the meteorological buoy: *TDR1* Tahoe Raft 1. **b** Finite-element grid representation of Lake Tahoe showing 50 m perimeter resolution; 250 m resolution within 1 km of shore; 500 m resolution farther offshore. **c** Emerald Bay bathymetry. Temperature depth sites: *EBS* Emerald Bay Sill, *EBT* Emerald Bay Tip. **d** Finite-element grid representation inset of Emerald Bay

the sediment). The instrument package is cabled to a dock-mounted Campbell Scientific CR1000 data-logger that averages 6-s measurements into 30-s records. Atmospheric pressure measurements, simultaneously recorded by barometers on each dock, are subtracted from CTD-measured pressure data to remove the atmospheric signal from the lake level estimates. Pressure measurements on the CTD are accurate within 0.001% of the raw pressure signal (RBR Limited, http://www.rbr-global.com). At 2-m depth, with a lake surface elevation of about 1897 m, the CTD measures raw pressure values near 10 dBar; pressure measurements are assumed accurate to 10^{-4} dBar (better than 0.1 mm of freshwater). The C3 measures chlorophyll-*a* fluorescence (fChl), colored-dissolved organic matter fluorescence (fCDOM), and turbidity. Bio-fouling of these measurements is minimized by wipers on the optical faces of the instruments.

This study focuses on NS data recorded from 7 February to 14 March, 2018, a 5-week unstratified period that included several wind events. The NS measurements are supplemented by data from three separate deployments of RBR duet temperature–depth (TD) units at other locations of interest. The TD's sampled temperature and pressure at 1 Hz and with an accuracy comparable to that of the NS stations. Barometric pressure, recorded at the NS stations, was subtracted from the TD data prior to performing any analyses.

A TD was deployed inside of the Tahoe City marina from October 17–31, 2017. The marina is bounded by shoreline to the west/northwest, a permeable rock-crib wall to the southwest, an impermeable seawall to the east/southeast, and has a 25 m opening for boat passage to the northeast. The Tahoe City NS station is situated immediately outside of the southwest marina boundary (TC, Fig. 1a); the TD was deployed inside of the marina, mounted to a weight on the lakebed, on the opposite side of the marina boundary from the TC NS station.

A TD was deployed from December 1–12, 2018 in the wetland formed at the confluence of the Upper Truckee River and Lake Tahoe (UTR; Fig. 1a). The instrument was mounted to a weight on the riverbed at 0.5 m depth in the main branch of the UTR, about 300 m upstream from the lake. The dynamics of the UTR wetland are driven by seasonal snowmelt and by lake level, the latter capable of varying by over 2 m. At the time of the deployment, UTR inflow into the wetland averaged 1.1 m^3/s, typical for December but only about 42% of the annual average flow (2.6 m^3/s). After an unusually wet winter in 2016–2017, the lake level in December was about 90 cm above the 2000–2017 average.

From March 1 to March 14, 2018 two TD's were deployed in Emerald Bay, one at the tip of the bay and the other on the shallow sill separating the bay from the main basin (EBT and EBS; Fig. 1c). The EBS deployment also included a Mini-DOT optical dissolved oxygen (DO) sensor sampling at a 1-min interval. No flow measurements were recorded during this TD deployment. However, three-dimensional flow data from a previous acoustic Doppler velocimeter deployment (ADV) were available. A Nortek Vector ADV (http://www.nortekusa.com) was deployed at EBS from 9 February to 22 February 2012. The probe was positioned approximately 15 cm above the sandy sill and sampled in 8 Hz bursts for 1-min intervals every 5 min. The east–west, north–south, and vertical components of the bursts were averaged into single, 5-min values in each of the three spatial dimensions.

Meteorological data were recorded from the TDR1 buoy (Fig. 1a) maintained by the UC Davis Tahoe Environmental Research Center (TERC). Table 1 summarizes instrument deployment dates and sampling regimes.

Finite-element model

The finite-element code of Rueda and Schladow (2002) was employed to model the expected spatial expression and periods of the barotropic seiche modes in Lake Tahoe. Following Hamblin (1982), the model sets up an eigenvalue solution to the non-rotational representation of periodic lake level fluctuations:

$$\frac{\partial}{\partial x}\left(h\frac{\partial \zeta}{\partial x}\right)+\frac{\partial}{\partial y}\left(h\frac{\partial \zeta}{\partial y}\right)+\left(\frac{\omega^2}{g}\right)\zeta=0. \quad (1)$$

In Eq. (1), x and y represent two-dimensional direction along the lake surface, h is the spatially varying basin depth,

Table 1 Summary of field deployments

Deployment	Dates	Sampling rate	Relevant measurements
Nearshore monitoring stations (NS)	7 February to 14 March 2018	30 s	Pressure, BP, temperature, turbidity, fChl-a, fCDOM
Tahoe City marina TD (TCM)	17–31 October 2017	1 s	Pressure, temperature
Upper Truckee River wetland TD (UTR)	1–12 December 2017	1 s	Pressure, temperature
Emerald Bay TD's (EBT and EBS)	1–14 March 2018	1 s	Pressure, temperature
Emerald Bay Sill ADV (EBS)	9–22 February 2012	5 min (8 Hz for 1 min)	3-D flow velocity; 15 cm above bottom
Meteorological buoy (TDR1)	Throughout study	10 min	Wind speed and direction

and ζ is surface displacement from equilibrium. Treating surface seiches as shallow-water waves, and assuming a characteristic depth scale equal to the average lake depth (300 m), we estimate the Rossby radius of deformation as the ratio of the shallow-water wave celerity ($\sqrt{gh}$) and the Coriolis parameter ($f = 10^{-4}s^{-1}$), equal to about 550 km. As the maximum length scale of the lake is 30 km, rotational effects on barotropic oscillations in Lake Tahoe can be considered minimal.

Lake bathymetry was discretized into triangular elements from the 10-m resolution digital elevation model produced by the United State Geological Survey (Gardner et al. 2000). Elements were generated by applying Delaunay triangulation to a mixed spatial resolution grid, with 50 m node spacing along the shoreline, 250 m node spacing between the shoreline and a boundary 1000 m from shore, and 500 m node spacing farther offshore (Fig. 1b, d). This technique enabled resolution of the complex shoreline—in particular the narrow mouth of Emerald Bay (Fig. 1d)—while limiting computational cost associated with a uniformly high-resolution grid. Finer grid resolution did not yield noticeable change to the calculated spatial structure of the seiches; triangulation of uniform 250 m and 50 m grids only affected estimated periods by a few seconds or less (less than 0.1%).

Analytical methods

Time-series analyses were performed using a multi-taper spectral analysis toolbox, Chronux (Bokil et al. 2010; http://chronux.org), initially developed for neuroscience applications. This toolbox implements Thomson's multi-taper methods (Emery and Thomson 2001), used successfully for spectral analysis in many fields, including physical limnology (Cimatoribus et al. 2018). Compared to segment-averaging techniques and wavelets, multi-taper spectral methods minimize frequency leakage (van Vugt et al. 2007), a useful property when isolating unique signals of similar frequencies. A time–bandwidth product, $NW = 5$, with $K = 2NW - 1$ tapers, was used for calculating the power spectral density of the pressure signals described below. For time-varying coherence and phase-lag calculations, we increased the time–bandwidth product and number of tapers ($NW = 20$; $K = 2NW - 1$), and used a 48 h moving window, with 50% overlap, to increase confidence at the expense of some frequency resolution.

Data from the NS stations were analyzed to verify the accuracy of the model predictions for the first six main-basin seiche modes. The frequency distributions of power spectral density (PSD) in the NS pressure signals were compared to the seiche frequencies and nodal distributions predicted by the model. Spectral power is expected to be present at anti-nodal sites and absent at nodal sites for a given seiche mode.

For each seiche mode, spectral peaks in the NS pressure signals were further verified as seiche-related using coherence and phasing analysis between a reference NS site and: (1) a site situated on the same antinode as the reference site; (2) a site situated on an opposing antinode as the reference site; and (3) a nodal site. For basin-scale oscillations, coherence is expected between the reference site and (1) and (2), but not necessarily (3). The reference site and (1) are expected to be in phase, and the reference site and (2) are expected to be out of phase. Sites were selected qualitatively based on the nodal distributions predicted by the model.

Coherence analysis between NS pressure signals and NS water quality signals was performed to explore the potential relevance of barotropic oscillations to littoral water quality. Coherence analysis highlights shared frequency signatures between signals, regardless of the phasing of these signatures (Emery and Thomson 2001).

The time-varying amplitude of barotropic oscillations was estimated by band-pass filtering the NS pressure signals for each seiche mode using a second-order Butterworth filter (Emery and Thomson 2001). Seiche-specific frequency bands were centered on observed seiche frequencies and had 0.0385 Hz (26 s period) windows to minimize energy leakage from other seiche modes of similar frequencies. A 1-h windowed Hilbert transform was used to calculate the envelopes of the band-pass filtered signals, which is analogous to calculating the modulation of oscillatory amplitudes.

Spectral and amplitude analyses were similarly performed on TD data from the marina, wetland, and bay deployments. The presence of surface seiche oscillations in these semi-enclosed peripheral water bodies are used to estimate the potential for seiche-driven exchange flow with the main-basin.

In Emerald Bay, model results for the zeroth-mode were evaluated using both the EBT and EBS pressure data. Data from the ADV deployment on the Emerald Bay Sill were decomposed into cross-sill (30° clockwise from north; into/out-of-bay) and along-sill (120° clockwise from north) components. Spectral and amplitude analyses of the velocity components were used to explore the role of the main-basin and bay mode surface seiches in driving exchange flow between Emerald Bay and Lake Tahoe.

Results

Finite-element model

Model results detail the theoretical nodal distributions and periods for the first six barotropic seiche modes in Lake Tahoe (Figs. 2, 3). Given the complex nodal patterns predicted by the model, we denote the modes in order of descending period rather than specifying the modal order of

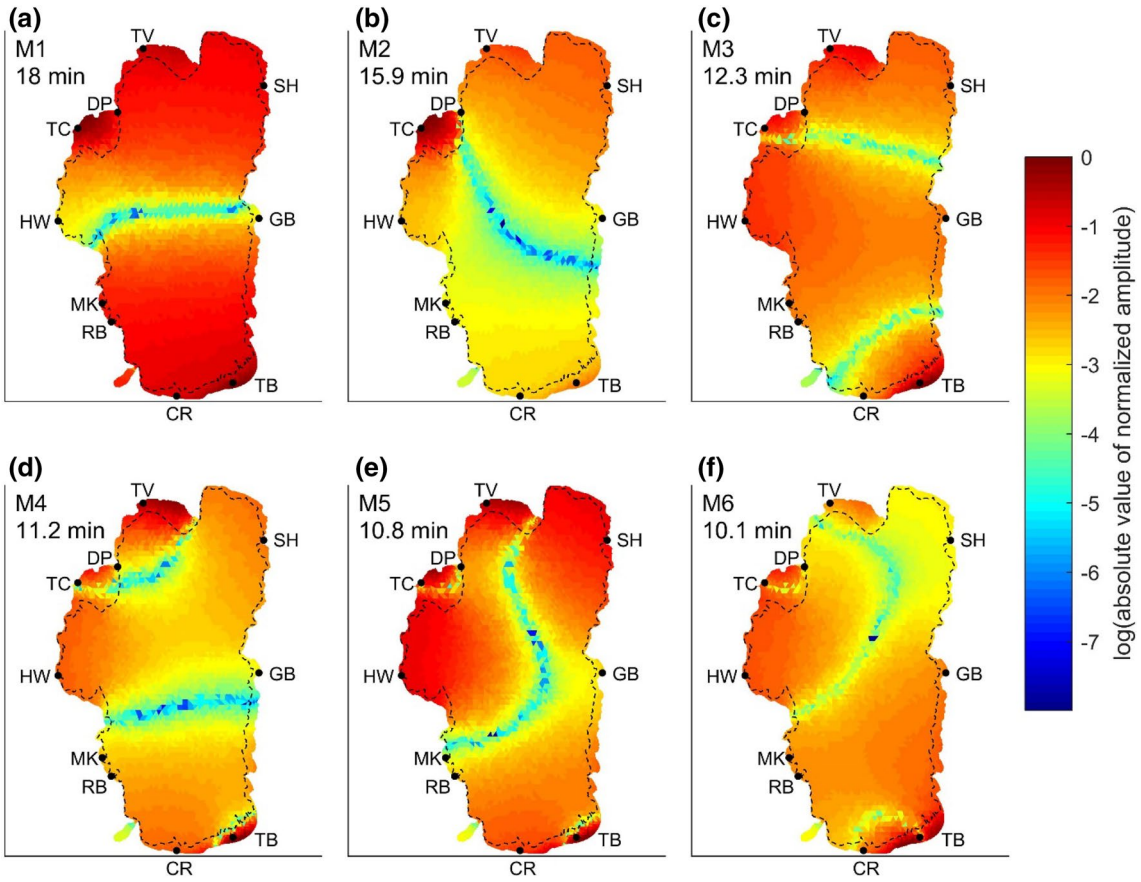

Fig. 2 Logarithm of modeled relative seiche amplitudes for the first six main-basin modes. **a–f** The oscillation period for each mode and the corresponding nodal structures. Color contours show $\log_{10}$ (absolute value of normalised amplitude) for each mode. Blue colors correspond to nodal lines where oscillations are minimal; red colors correspond to antinodes where lake-level oscillations are expected to be maximal. Black dots correspond to nearshore station sites as shown in Fig. 1a. Dashed line shows the 25-m isobath in the main basin for reference (color figure online)

specific longitudinal or latitudinal modes. In Fig. 2, a log-scale representation of the model results, cool (blue/green) colors indicate minimal oscillatory amplitudes, the nodes, associated with a given seiche mode; warm (red/orange) colors indicate antinodes, areas of maximum expected fluctuations in lake level. Figure 3, a normalized linear representation of the results, highlights areas of maximal seiche-driven surface displacements. Associated flow velocities should be greatest where lake-surface gradients are strongest, as shown by rapid transitions from bright blue or red to pale green in Fig. 3; for most modes, maximum seiche-driven velocities are expected on the shelves near Tahoe City, Tahoe Vista, and Timber Cove.

Periods associated with the first six modes range from 18.0 to 10.1 min, descending from M1 to M6. For all modes, the model predicts maximum relative seiche amplitudes on the shelves near Tahoe City, Tahoe Vista, and/or Timber Cove (Fig. 3). At all modes higher than the fundamental M1, complex nodal distributions appear to be affected by shelf features, particularly at higher modes (Figs. 2, 3).

Spectral decomposition of nearshore pressure signals

Spectral representation of the pressure signals from the ten NS stations reveals the periods of the resonant barotropic oscillations, and confirms their model-predicted spatial expression. Figure 4 shows the power spectral density (PSD) of NS pressure data across the band associated with expected seiche periods (6–34 min). Site-to-site comparison of spectral peaks reveals consistent signal frequencies, confirming that these peaks represent basin-scale processes. The periods associated with these peaks are close to those predicted by the model (Table 2); dashed lines and labels in Fig. 4 correspond to observed seiche periods.

Collectively, site-specific spectral peaks offer insight into the spatial distribution of seiche expression. For a given seiche mode and associated frequency, we expect to see spectral power in the pressure signal at anti-nodal sites, and we expect an absence of spectral power at nodal sites. Stronger peaks are expected in the areas of amplified

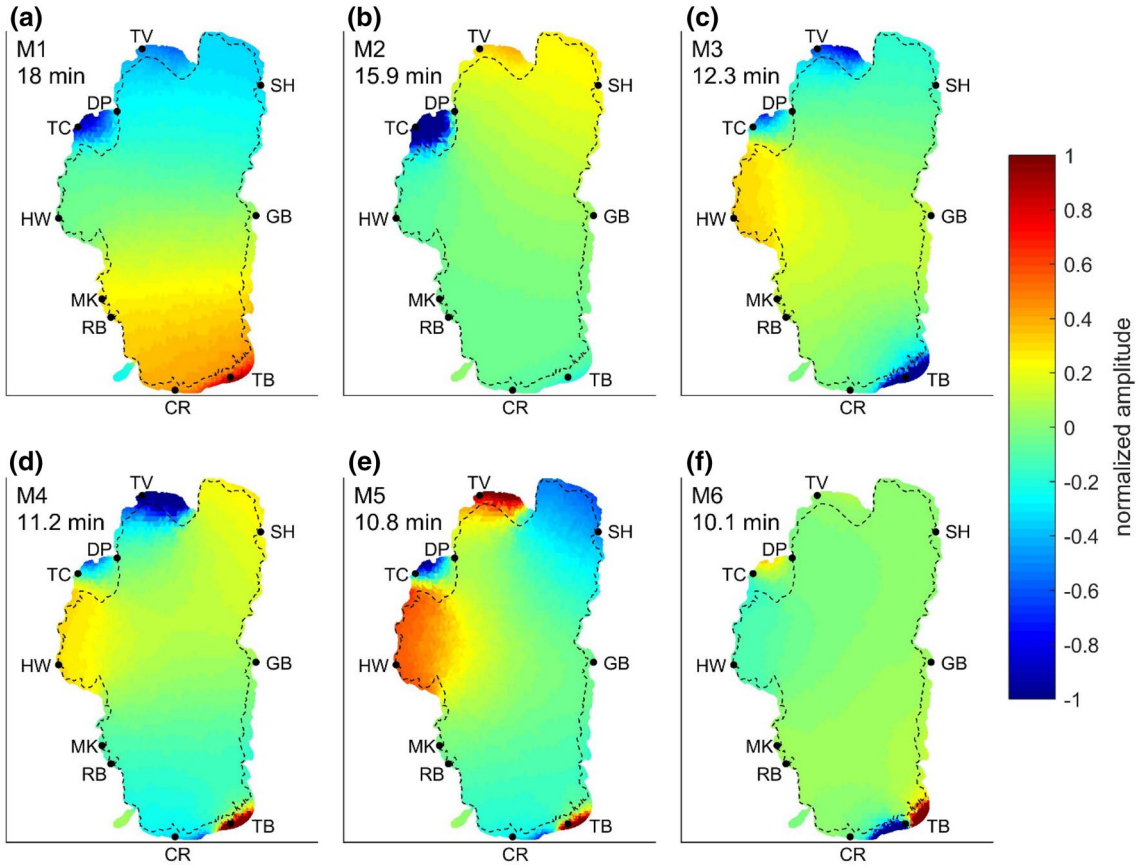

Fig. 3 Modeled relative seiche amplitudes for the first six main-basin modes. **a–f** The oscillation period for each mode and highlight areas of maximal oscillatory amplitude. Color contours show the normalized amplitude of lake-surface oscillations for each mode. Warm (reds) and cool (blues) colors correspond to elevated and depressed lake surface elevation respectively. The sign of lake-level fluctuations alternates with each half-oscillation of the given seiche; contour colors are interchangeable but serve to delineate opposing anti-nodal areas. Black dots correspond to nearshore station sites as shown in Fig. 1a. Dashed line shows the 25-m isobath in the main basin (color figure online)

seiching shown by blue or red colors in Fig. 3. The agreement between model-predicted nodal distributions and observed oscillations is excellent. The M1 signal is present at all NS sites with the exception of Homewood and Glenbrook (Figs. 4d, f), as predicted by the modeled nodal distribution (Fig. 2a). Consistent with the modeled spatial pattern shown in Figs. 2b and 3b, Tahoe City data include a strong M2 signal (Fig. 4d), and this signal is otherwise only weakly present at Tahoe Vista, Sand Harbor, and Timber Cove (Fig. 4f, g, i). The M3 signal is clearly present at Timber Cove (Fig. 4i), as predicted by the model (Fig. 3c), but is otherwise mostly absent from data at other NS sites. Particularly strong spectral peaks at Tahoe City (M1 and M2) and Timber Cove (M1 and M3) are consistent with model-predicted seiche amplification at these shelf sites.

At modes M3–M5, site-specific spectral peaks continue to agree with model-predicted nodal distributions. The model predicts M6 expression at Tahoe City and Timber Cove (Fig. 3f), but a corresponding spectral peak is only present at Tahoe City. At higher modes, where nodal patterns become particularly complex, accurate prediction of seiche structure may be limited by the model grid resolution. Lower period (higher frequency) spectral peaks are apparent in the data at Tahoe City, Tahoe Vista, Sand Harbor, and Camp Richardson; for brevity, analysis of these higher modes is left out of this study.

Nearshore seiche amplitudes

Intuitively, relative site-to-site seiche amplitude is correlated with the mode-specific anti-nodality at a given locale. Figure 5 shows the amplitudes of the pressure signals after individually band-pass filtering for the six seiche modes. Signals with average amplitude greater than 0.3 cm are shown in color, revealing dominant modes at each station that are consistent with the spectral peaks shown in Fig. 4. The fundamental M1 seiche is present at amplitudes of 0.5–2 cm at all but the nodal sites. The three "shelf sites"—Tahoe City,

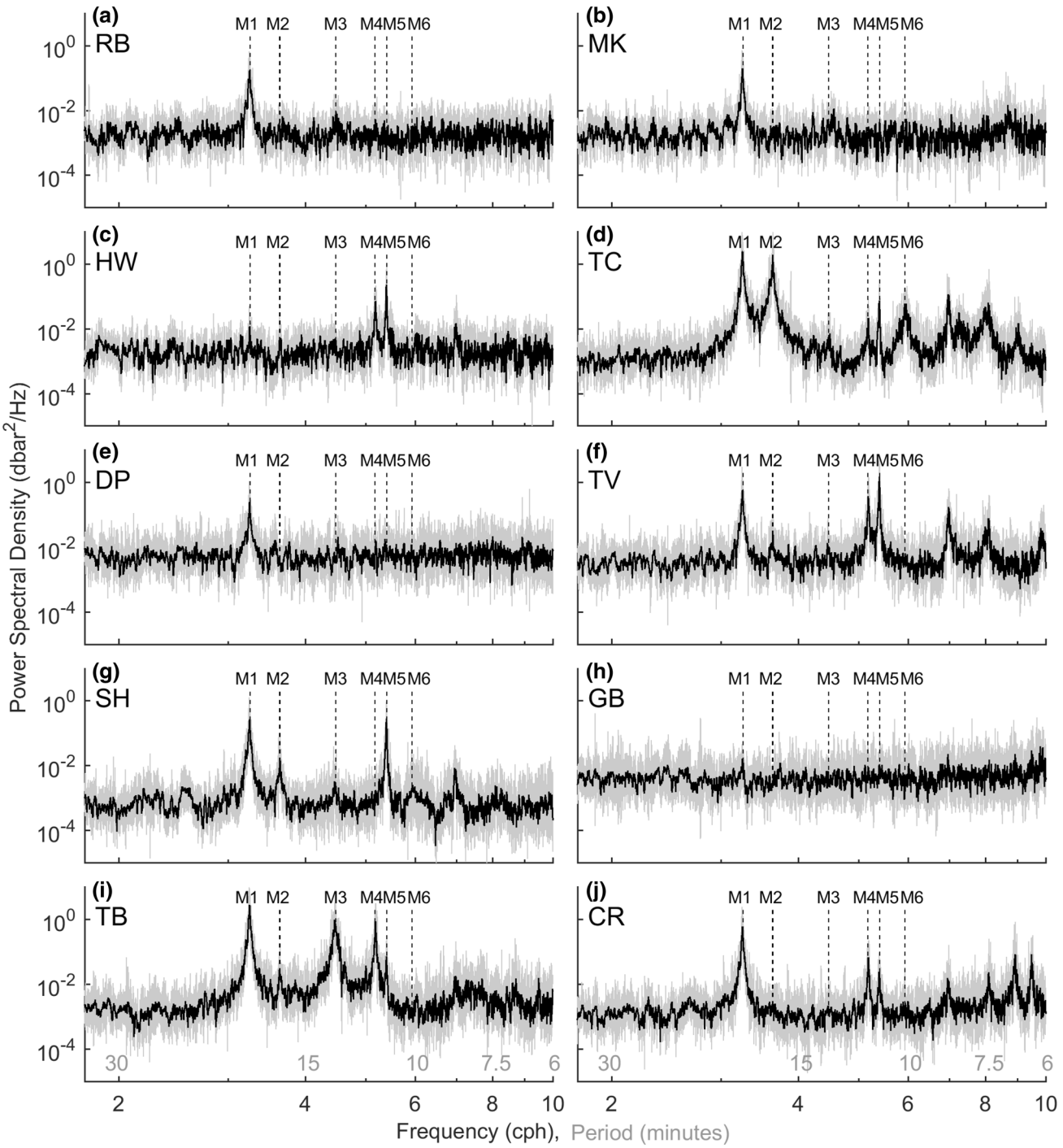

Fig. 4 Spectra of lake-level signals at each nearshore station over the period 7 February to 14 March, 2018. **a** Rubicon; **b** Meeks; **c** Homewood; **d** Tahoe City; **e** Dollar Point; **f** Tahoe Vista; **g** Sand Harbor; **h** Glenbrook; **i** Timber Cove; **j** Camp Richardson. Grey bands show the 95% confidence band. Dotted lines and mode labels correspond to observed periods shown in Table 2

Tahoe Vista, and Timber Cove—include the most dynamic barotropic "weather". These sites all include three seiche modes with average amplitudes greater than 0.3 cm, and all include at least one mode with average amplitude exceeding 1 cm. The M1 has average amplitudes of 1.2 and 1.3 cm, and peak amplitudes greater than 5 cm, at Tahoe City and Timber Cove, respectively. The M2 has a similar average and peak at Tahoe City. The M3 is uniquely expressed at Timber Cove, with amplitudes rivaling those of the M1 at the other shelf sites.

Table 2 Modelled and measured seiche periods

Seiche mode	Modeled period (min)	Measured period (min)
EB-M0	29.5	30.5
M1	18.0	18.4
M2	15.9	16.5
M3	12.3	13.4
M4	11.2	11.6
M5	10.8	11.1
M6	10.1	10.1

The amplitudes of all of the seiche signals vary in time in response to patterns in excitation and subsequent damping. Band-pass filtering (pass-band 2–6 cph) of 30-s barometric pressure data (on-deck at nearshore stations) shows greater magnitude pressure fluctuations in the seiche-frequency band preceding the periods of amplified seiching (Fig. 6). These high-frequency pressure oscillations generally accompanied drops in barometric pressure, indicative of the arrival of atmospheric fronts. The small-amplitude excitation observed during the study period may have been due to resonant patterns in atmospheric pressure forcing. However, a detailed study of excitation and damping mechanisms is beyond the scope of this investigation.

Pressure-coherence and phase-lag analysis

Coherence and phase-lag analysis between pressure signals from NS sites further confirms the model-predicted seiche patterns. Figure 7 shows phase-lag between the mode-specific pressure signals at a reference site and a site on the same antinode (black), a site on an opposing antinode (red), and a nodal site (light-grey dashed). Table 3 outlines the site-to-site relationships used to generate

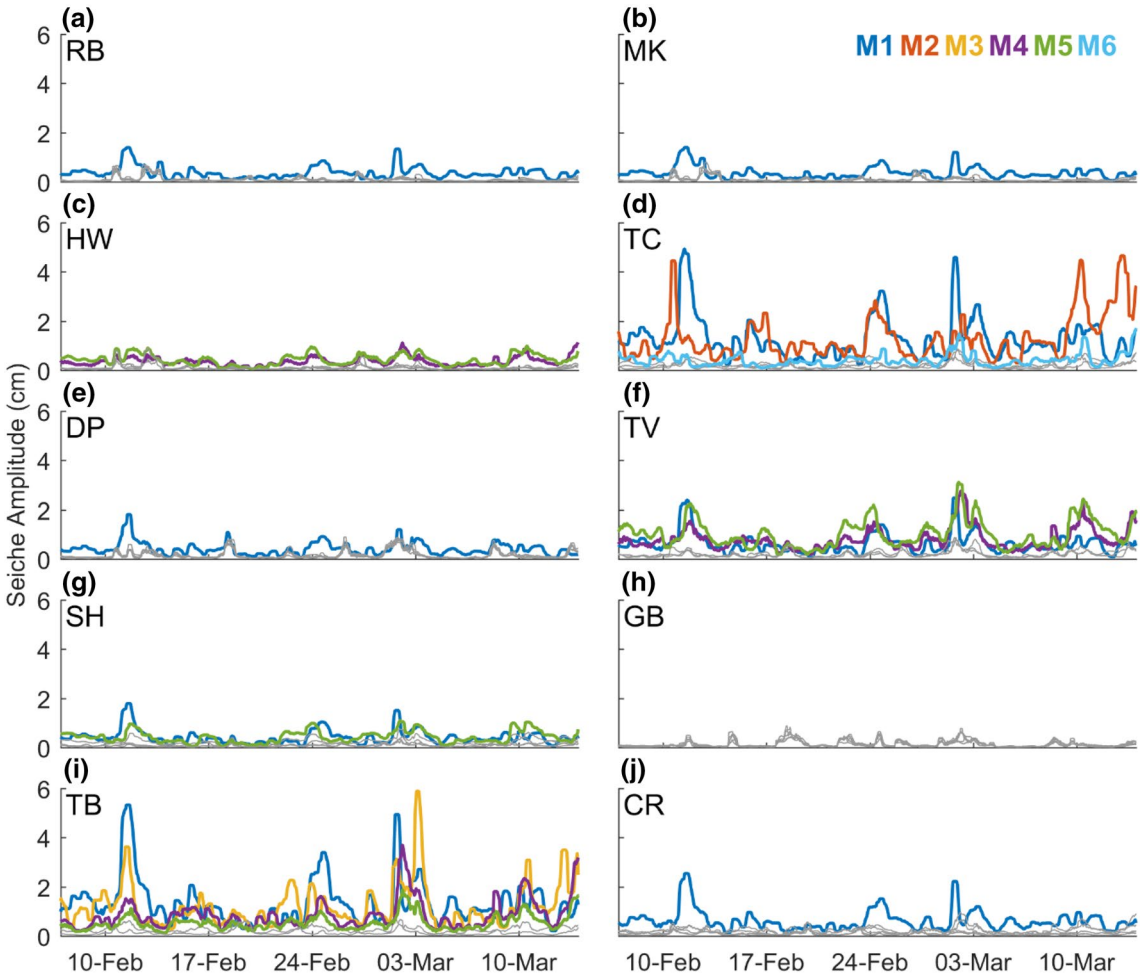

Fig. 5 Time-varying seiche amplitudes for each of the first six main-basin modes at each of the nearshore stations. **a** Rubicon; **b** Meeks; **c** Homewood; **d** Tahoe City; **e** Dollar Point; **f** Tahoe Vista; **g** Sand Harbor; **h** Glenbrook; **i** Timber Cove; **j** Camp Richardson. Mode-specific colors shown on the M(X) labels in **b** apply to all subplots; lines shown in grey if average amplitude is less than 0.3 cm. Data are smoothed with a 6-h moving-median filter for clarity

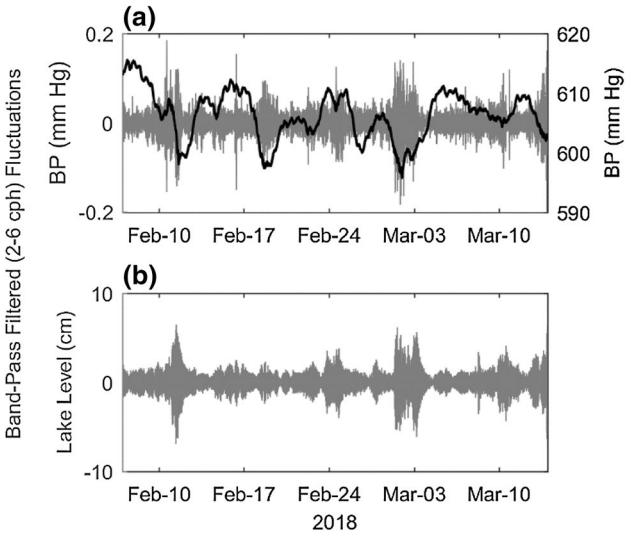

Fig. 6 **a** Barometric pressure (BP) signal (black) and band-pass filtered (2–6 cph) barometric pressure fluctuations (grey) measured on-deck at Timber Cove. **b** Band-pass filtered (2–6 cph) lake level signal at Timber Cove nearshore station

Fig. 7. For modes 1 through 5, pressure signals from sites on shared mode-specific antinodes are in-phase and signals from opposing mode-specific antinodes are out-of-phase, and both show statistically significant coherence (> 99% confidence; not shown). This result supports model-predicted nodal distributions for M1–M5 by confirming that seiche-driven lake-level rise occurs simultaneously at multiple locations on one side of the oscillatory node while lake-level falls at a site on the opposite side of the node (Fig. 7a–e). Phase-lag analysis for the M6 revealed no clear relationships between pressure oscillations at the selected sites (Fig. 7f), likely because: (1) the distribution of NS sites did not capture M6 antinodes; (2) this signal is only weakly expressed in the lake; and/or (3) model accuracy decreases at higher modes due to grid resolution.

Pressure–water quality coherence analysis

Coherence analysis revealed limited relationships between seiche-related pressure fluctuations and water quality fluctuations at individual nearshore sites. No coherence was found between pressure signals and fChl, fCDOM, or turbidity signals at any site. However, two of the "shelf sites", Tahoe City and Timber Cove, show pressure–temperature coherence at specific modes; M1, M2, and M6 at Tahoe City, M1 and M3 at Timber Cove (Fig. 8). While this coherence is inconsistent, sometimes disappearing for days at a time, it stands out from the complete lack of significant water quality coherence at all other sites. Weak but clear spectral peaks at these periods in the temperature signals from these sites confirm the relationship between lake level fluctuations and near-bottom temperature (not shown).

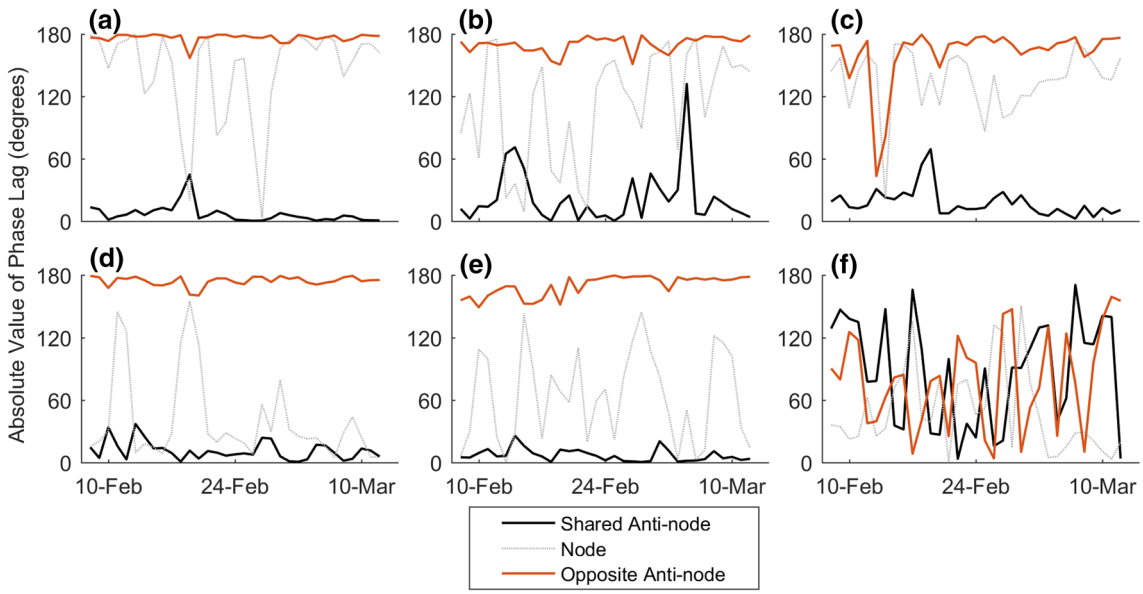

Fig. 7 Absolute value of phase-lag between the lake level signals at a reference site and: (1) a site on a shared antinode (black); (2) a nodal site (light grey dashed); and (3) a site on an opposing antinode (red), for each of the six main-basin seiche frequencies. **a–f** Correspond to modes M1–M6. Reference, shared-antinode, nodal, and opposing-antinode sites for each mode are shown in Table 3. Phase lags of 0° and 80° correspond to completely in-phase and completely out-of-phase signals, respectively (color figure online)

Table 3 Reference sites for inter-site coherence and phase-lag analysis

Seiche mode	Reference site	Shared anti-node	Opposing anti-node	Node
M1	Tahoe Vista	Sand Harbor	Timber Cove	Glenbrook
M2	Tahoe City	Homewood	Sand Harbor	Dollar Point
M3	Timber Cove	Sand Harbor	Homewood	Camp Richardson
M4	Timber Cove	Homewood	Camp Richardson	Glenbrook
M5	Homewood	Tahoe Vista	Sand Harbor	Meeks
M6	Camp Richardson	Timber Cove	Homewood	Sand Harbor

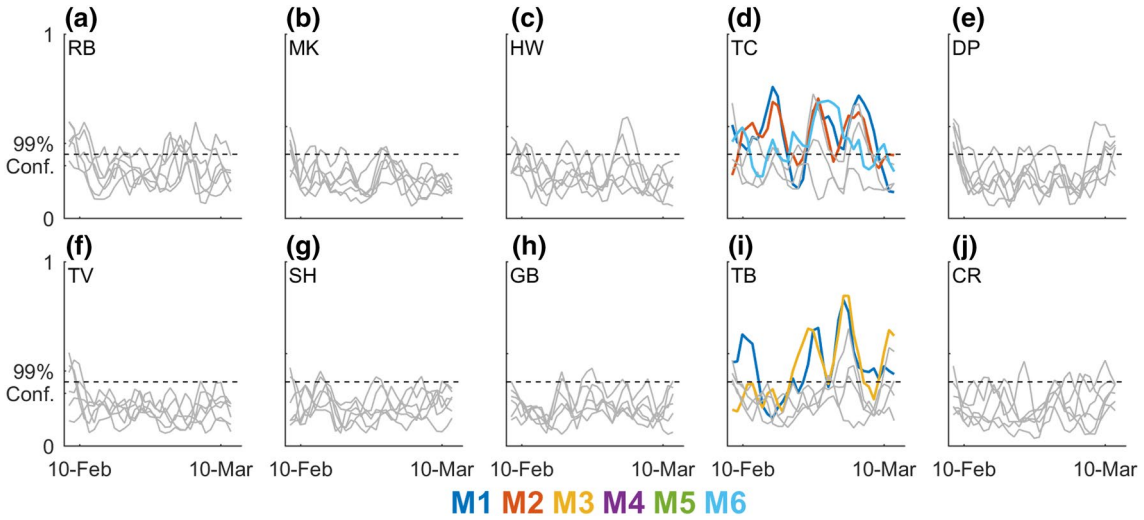

Fig. 8 Coherence between temperature and pressure (T–P) signals at **a** Rubicon; **b** Meeks; **c** Homewood; **d** Tahoe City; **e** Dollar Point; **f** Tahoe Vista; **g** Sand Harbor; **h** Glenbrook; **i** Timber Cove; **j** Camp Richardson. Dashed horizontal lines show the 99% confidence limit ($p = 0.01$). Where mode-specific T–P coherence is statistically significant (greater than 99% confidence) for at least 60% of the study period, lines are shown in colors corresponding to each mode as denoted by the bold, colored legend at bottom. Mode-specific coherence is shown as a thin grey line if coherence is statistically significant for less than 60% of the study period

Seiche expression in semi-attached water bodies

Water surface oscillations at main-basin seiche frequencies are present in semi-enclosed water bodies connected to Lake Tahoe's main basin (Fig. 9). The pressure signal recorded inside of the Tahoe City Marina shows spectral peaks similar to those present outside of the marina at the TC nearshore station (Fig. 9a), and at comparable amplitudes (not shown). The M1, M3, and M4 oscillations, present at nearby NS Timber Cove, are apparent in the UTR pressure signal, several hundred meters upstream from the lake perimeter (Fig. 9b). However, the magnitudes of the seiching in the wetland (0.5–2 cm) are smaller than those on the Timber Cove shelf (2–4 cm); it is unclear whether this difference is due to magnification on the shelf or damping within the wetland. The main-basin fundamental seiche (M1) is not only present at the shallow sill of Emerald Bay (Fig. 9c) but penetrates into the far end of the bay (Fig. 9d) as predicted by the model (Fig. 2a).

In addition to the influence of main-basin seiche modes, a bay-mode seiche (M0), predicted by the model (Fig. 10), drives a longer-period oscillation that is strongly expressed within the bay (Fig. 9c, d) but is nearly undetectable in the main-basin (Fig. 4). The measured period of this oscillation is 30.5 min, close to the model-predicted period of 29.5 min (Table 2).

Analysis of M0 lake-level fluctuations at EBS and EBT reveal the expected bay-mode structure (Fig. 11a); amplitudes on the sill are very small, while amplitudes at the tip of the bay are significantly greater (regularly exceeding 1 cm). Lake-level fluctuations associated with the M1 were similar at both EBS and EBT (Fig. 11b), as would be expected at neighboring anti-nodal sites for the whole-lake fundamental seiche mode.

Since neither the M0 nor M1 seiches include nodes inside of Emerald Bay, both modes necessarily drive exchange flow with the main lake basin. Strong spectral peaks in the EBS temperature data, at both the M0 and M1 frequencies, point to the expected exchange (black line; Fig. 11c). The

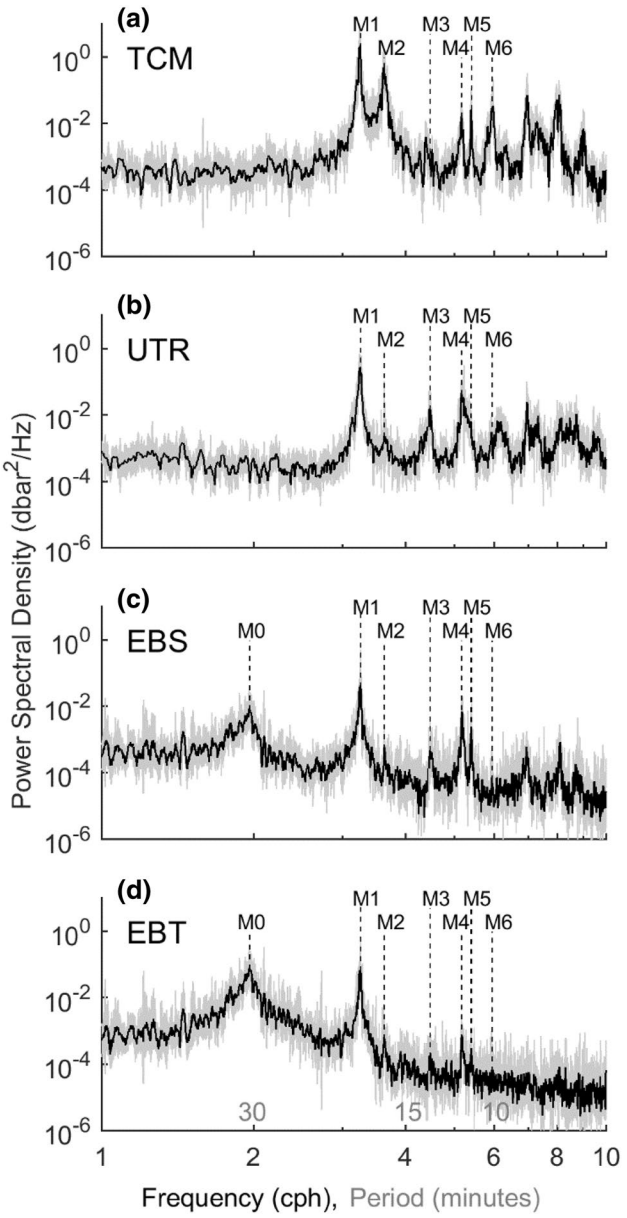

Fig. 9 Spectral representation of lake-level signals from the four supplemental temperature-depth sensor deployments. **a** Tahoe City Marina; **b** Upper Truckee River wetland; **c** Emerald Bay Sill; **d** Emerald Bay Tip. Grey bands show the 95% confidence interval. Dotted lines and mode labels correspond to observed periods shown in Table 2

lack of spectral power at either M0 or M1 frequencies in the EBT temperature data (grey line; Fig. 11c) supports the hypothesis that temperature fluctuations in the EBS signal are related to seiche-driven exchange with the main-basin. M0 and M1 spectral peaks in the DO concentration signal at the EBS site hint at seiche-driven pore-water flow across the shallow Emerald Bay Sill (not shown). However, the amplitudes of associated oxygen concentration fluctuations are on the order of only 10^{-1} mg/l (a fraction of a percentage of saturation), nearly negligible variability in the consistently well-oxygenated water. If surface seiches are driving flow through the Emerald Bay Sill, the persistence of the seiching may prevent oxygen depletion in the pore water.

Historic flow data, recorded by an ADV at the EBS site in 2012, confirm the importance of the 0.5–1.5 cm surface seiches to cross-sill flows between Emerald Bay and Lake Tahoe, and thus to seiche-related temperature fluctuations on the Emerald Bay Sill. The ADV data include cross-sill velocity fluctuations of 1–5 and 1–7 cm/s at M0 and M1 frequencies respectively; along-sill flows are nearly negligible in comparison (Fig. 12a, b). Consistent with these band-pass filtered velocity signals, spectral power at the M0 and M1 frequencies is present in the cross-sill flow data and absent in the along-sill flow data (Fig. 12c). These seiche-related peaks dominate the spectral representation of the signal across a broad range of periods, from the Nyquist frequency (6 cph) through frequencies corresponding to internal-wave periods (order of 10^1–10^2 h). A sensitivity analysis of the selected cross-sill angle confirms the principle axis of seiche-driven cross-sill flows near 30°.

Discussion

Modeled and observed patterns in basin-scale surface oscillations

The complex nodal structures of Lake Tahoe's surface seiches, shown in Figs. 2 and 3, and validated in Figs. 4 and 7, emphasize the importance of accounting for basin morphometry when estimating seiche structures and periods, even in lakes with comparatively simple single-basin bathymetry.

Ichinose et al. (2000) applied Merian's formula to estimate the periods of the fundamental latitudinal and longitudinal surface oscillations of Lake Tahoe, assuming a rectangular basin (35.4 km × 19.2 km) and constant depth (500 m). These simplified spatial patterns correspond most closely to the M1 and M2 structures shown in Fig. 2a, b. The Merian's formula estimate of 16.9 min for the fundamental latitudinal (M1-like) seiche is close to the observed value of 18.4 min, and to our modeled value of 18 min. However, we observed no seiche pattern that corresponds to the fundamental longitudinal seiche (straight node running north–south through the center of the lake) discussed by Ichinose et al. (2000). This nodal geometry may be best approximated by our M2 model result (Fig. 2b), but the fundamental longitudinal period of 9.1 min, approximated by Ichinose et al. (2000), is far from our observed and modeled values of 16.5 and 15.9 min.

At higher modes, accounting for lake morphometry becomes critical to untangling complex and overlapping

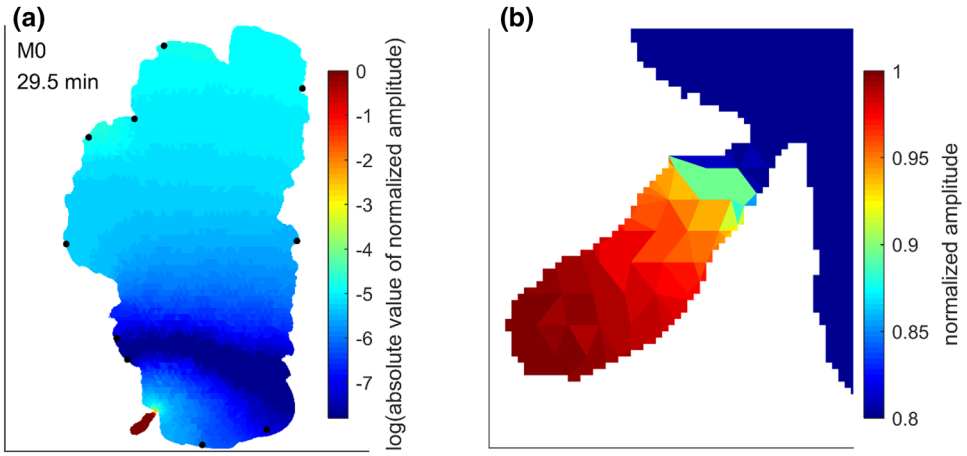

Fig. 10 Finite-element model result for the Emerald Bay zeroth mode (M0) seiche. **a** Full-basin model results shown as $\log_{10}$ (absolute value of normalised amplitude). **b** Inset of Emerald Bay (as in Fig. 1d) showing linear-scale normalized amplitude to highlight seiche structure within the bay (note the limited range of color scale). Blue colors correspond to areas where oscillations are minimal; red colors correspond to antinodes where lake-level oscillations are expected to be maximal. Black dots in **a** correspond to nearshore station sites shown in Fig. 1a (color figure online)

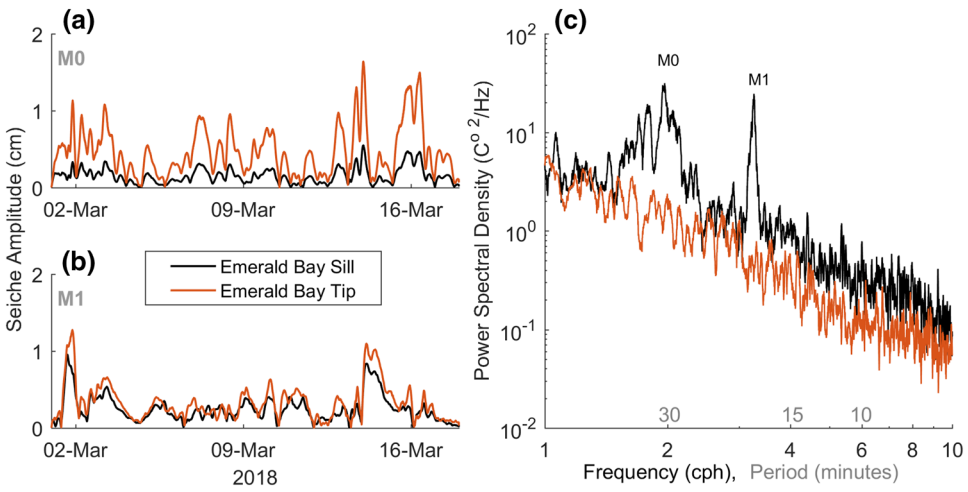

Fig. 11 Time-varying seiche amplitudes (pressure) and spectral representation of temperature signals at the Emerald Bay Sill (black) and Tip (red). **a** Amplitude of the EBS and EBT pressure signals band-pass filtered to the M0 frequency band. **b** Amplitude of the EBS and EBT pressure signals band-pass filtered to the M1 frequency band. **c** Spectral representation of EBS and EBT temperature signals (color figure online)

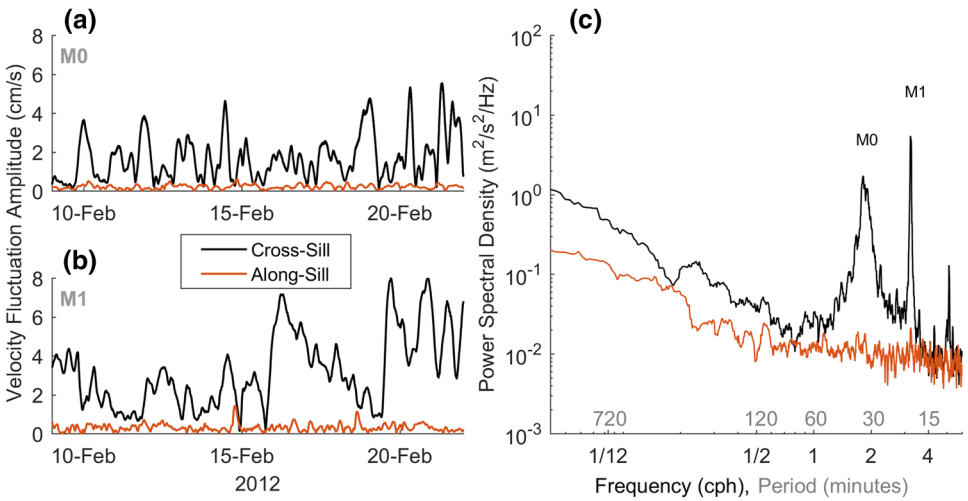

Fig. 12 Amplitude and spectral representations of the cross-sill (black) and along-sill (red) components of velocity data from the Emerald Bay Sill. **a** Cross-sill and along-sill velocity components band-pass filtered to the M0 frequency band. **b** Cross-sill and along-sill velocity components band-pass filtered to the M1 frequency band. **c** Spectral representation of the cross-sill and along-sill velocity components (color figure online)

seiche patterns. Both the model results (Figs. 2, 3) and the observed data (Figs. 4, 5) show complex nodal patterns focused around shallow shelves. The magnitude of seiche oscillations is greater on shelves, both for the fundamental and for the higher modes (Figs. 3, 5). Even the comparatively simple M2 nodal structure focuses seiche expression on the shelf at Tahoe City (Figs. 2a, 3a, 4d); the M2 is only very weakly expressed at any other site, as predicted by the model. Without model results that take into account the effect of the Tahoe City shelf, an experimental study of the lake might conclude that there is no measurable longitudinal single-node seiche, when, in fact, the M2 shows a strong, albeit spatially isolated, signal.

Our results also highlight the importance of properly resolving small scale features, such as the connections to adjoining bays. Sprague (2017) utilized the same model with a uniform 500-m grid. At this resolution, Emerald Bay was effectively modeled as an inlet, rather than as a semi-enclosed basin. This coarser grid properly resolved the M1–M3 seiche structures. However, nodal structures at higher modes were shifted in the absence of the co-basin effect of a well resolved Emerald Bay. Additionally, the zeroth-mode seiche, which plays a significant role in exchange between Emerald Bay and Lake Tahoe, was not resolved. These results are consistent with findings from Lake Huron by Schwab and Rao (1977), but are notable in that, compared to the relative size of Lake Huron's large adjoining bays to its main basin, Emerald Bay is very small relative to Lake Tahoe. Even seemingly negligibly small attached sub-basins can affect the resonant structure of main-basin barotropic oscillations.

The effectiveness of the modeling approach employed here, adopted from Rueda and Schladow (2002), has been established for decades (Hamblin 1982). Our model results, particularly well validated using a distributed network of high-frequency instruments, highlight two important points: (1) proper resolution of adjoining basins, even relatively small ones, is important to accurately predict seiche patterns and periods; (2) even lakes of simple, single-basin geometry can have surface seiches with complex nodal structures that are ignored by simple analytical approximations.

Relevance of surface seiches to littoral water quality processes

The results suggest that surface seiches may play a role in littoral water quality processes even when amplitudes are quite small. Pressure–water quality coherence is limited at most nearshore sites, but seiche-driven lake-level fluctuations are correlated with temperature fluctuations at the shelf sites, where seiche expression is most pronounced (Fig. 8). Seiche-temperature coherence could be due to benthic pore-water exchange and/or pumping onto and off of shallow shelves. Seiche amplitudes did not exceed a few centimeters during our study period (Fig. 4), but our analysis shows that they still drive measurable reversing-flow across the mouths of attached water bodies at the lake perimeter. In Lake Tahoe, these flows may take on relevance in a variety of contexts, including dispersion of invasive macrophytes, nutrient and sediment loading from attached wetlands, and control of invasive Asian clams.

There is little evidence of coherence between seiche-related pressure fluctuations and water quality fluctuations at most NS sites. This may not be surprising given the low velocities expected to be associated with this process; gradients of modeled surface displacements yield maximum main-basin velocity estimates on the order of 10^{-2} cm/s, assuming maximum seiche amplitudes of 6 cm (per observations). However, at Tahoe City and Timber Cove, shelf sites where we observed comparatively larger seiche amplitudes, there are periods of coherence between temperature and pressure (M1, M2, and M6 for Tahoe City; M1 and M3 for Timber Cove; Fig. 8), and matching peaks in the spectral representation of the temperature signal. These limited periods of coherence generally appear during days of calm conditions (low wind speeds; minimal wind-waves) when the seiche effects are less likely to be drowned out by other hydrodynamic motions. Pressure–temperature coherence suggests seiche-related pumping during these otherwise calm periods. However, longer-term data would be needed to link surface seiches to water quality fluctuations under specific seasonal and forcing conditions.

The relevance of nearshore hydrodynamics to pore-water flow and associated sediment–water nutrient flux is well established (Oldham and Lavery 1999; Precht and Huettel 2003; Janssen et al. 2005; Cyr 2012). Internal waves (Kirillin et al. 2009), deep-water upwelling (Cyr 2012), and surface wind-waves (Evans 1994; De Vicente et al. 2010) have been directly connected to sediment–water column exchange in lake littoral zones. Though surface seiche-driven pore water flow is likely very small relative to wind-wave flow (Precht and Huettel 2003), surface seiching is capable of playing a role in sediment–water column nutrient flux (Basterretxea et al. 2011). At Tahoe, this is likely limited to periods where other hydrodynamic processes are relatively calm.

In addition to affecting benthic biogeochemical processes, through-sediment pumping could influence the diffusion of groundwater constituents into the water column. Groundwater is a significant nutrient source in Lake Tahoe (Loeb and Goldman 1979), and has been shown to affect periphyton growth in Lake Tahoe's littoral zone (Naranjo et al. 2019).

Seiche-driven exchange flow between peripheral water bodies and the lake littoral zone is potentially significant, even at the low seiche amplitudes observed in Lake Tahoe. Main-basin seiche signals measured in attached marinas, wetlands, and bays (Fig. 9) indicate some level of exchange

with the main-basin. Unmodeled, higher-frequency pressure signals were present in the Tahoe City Marina and in the UTR wetland (Fig. 9a, b), potentially indicating the presence of zeroth-mode or intra-sub-basin oscillations that could also contribute to exchange flow. In theory, any semi-enclosed basin attached to Lake Tahoe has a resonant zeroth-mode that could drive reversing flows across its mouth. However, testing whether higher-frequency signals at TCM and/or UTR correspond to local zeroth-mode seiches is difficult given the complex and time-variable geometry of the marina and wetland respectively.

The presence of the dominant NS Tahoe City seiche modes (M1 and M2) in the Tahoe City Marina (Fig. 9a) suggests a similar presence in marinas at seiche antinodes at other locations around the lake. In small, shallow marinas, such as Ski Run Marina near Timber Cove, even water–surface oscillations on the order of 1 cm can represent significant volumetric flux (Hamblin 1998). Several of Lake Tahoe's marinas are impacted by invasive aquatic plants, and their spread has implications for recreation and the local economy (Eiswerth et al. 2000). Seiche-driven exchanges could be a factor in the spread of these plants to other parts of the lake.

The presence of main-basin seiche signals in the UTR wetland (Fig. 9b) is likely dependent on UTR discharge relative to lake level. During the period of our deployment (December 2017), lake level was close to a meter above average, and discharge was well below the spring snowmelt peak. As a result, the delineation between lake and wetland was less clear, and wetland residence time was likely above average. Under these conditions, the 1–2 cm seiche signal could represent a significant driver of exchange between the lake and the wetland. Estimating the flux of nutrients and other contaminants released to the lake can be almost impossible with a conventional stream gauge when net flow is near-zero but seiches drive exchange flows. By knowing a priori the characteristic frequency of the seiches, it is possible to implement water quality sampling at a frequency that captures both the incoming and outgoing flows, improving estimates of the net flux. During high-flow periods, seiche-driven lake-surface oscillations are likely irrelevant to lake-wetland exchange. The UTR watershed represents the primary source of suspended sediment to Lake Tahoe, and is a significant source of nutrients. Quantifying these loads in the face of complex wetland dynamics is challenging. Regardless of whether seiche effects are ultimately integrated into load estimates, the potential presence of surface seiche signals in UTR measurements should be considered.

Zeroth-mode seiches have nodes near the mouths of bays and antinodes at the far ends of bays. In coastal bays and harbors, this rising and falling of the water level in semi-enclosed basins drives exchange with the open ocean (Rabinovich 2009). In Lake Tahoe, the zeroth-mode seiche would drive exchange between Emerald Bay and the main-basin of the lake. As predicted from theory, the associated oscillations were found to be strongest at the tip of the bay (EBT; Figs. 9d, 11a), weak on the sill (EBS; Figs. 8c, 10a), and nearly undetectable in the main-basin (Fig. 4).

Oscillatory cross-sill flows at the M0 and M1 frequency bands dominated the near-bed velocity signal throughout the 2012 ADV deployment (Fig. 12). Spectral peaks in the EBS temperature and oxygen signals are in line with these seiche-driven oscillatory flows (Fig. 11c). However, it's unclear whether the reversing bay-lake boundary, presumably responsible for the seiche-water quality coherence, drives appreciable mixing between the two basins or simply shifts the boundary back and forth on the sill. In either case, these reversing flows could play an important role in through-sill flows, particularly during the unstratified winter period when internal waves are weak or absent. Through-sill flows are believed to have rendered gas-impermeable benthic barriers less effective at eradicating invasive bivalves on the sill (via hypoxification of the benthos) as oxygenation of the sediments occurred despite the overlying barrier. By contrast, such barriers were 100% effective at reducing oxygen when deployed at Lake Tahoe sites far removed from seiche nodes (Wittmann et al. 2012).

This exploration of surface seiche expression in Lake Tahoe offers a useful descriptive reference but may raise as many questions as it answers. Does seiche-induced pumping, suggested by our data, drive ecologically relevant pore-water flow in the littoral zone? If so, how might spatial variability in surface seiche expression drive variability in benthic ecology? How significant of a role do surface seiches play in driving exchange with water quality-impacted marinas? What are the implications for the dispersal of invasive macrophytes? Given the high frequency of surface seiche oscillations relative to baroclinic waves, do surface seiches only drive lateral excursions at comparatively insignificant length scales? With an eye to focusing this study on a robust descriptive analysis of Lake Tahoe's surface seiches, we leave these questions to future studies. The results of this analysis serve to underscore the relevance of barotropic oscillations in a setting where they might typically be ignored, and to offer a descriptive record for future research on Lake Tahoe.

Conclusions

Surface seiches in Lake Tahoe have complex nodal distributions despite the relative simplicity of the basin morphometry. The observed magnitudes of Tahoe's surface seiches were small (order of 10^0 cm) during the study period, and their variability was likely driven by atmospheric pressure oscillations, though we did not explore the

latter in detail. Littoral shelves amplify these oscillations and shape the locations of nodes.

While we observed limited direct coherence between surface seiches and littoral water quality, some pressure–temperature coherence suggests potential for seiche-induced pumping. This process may be relevant during calm conditions when other hydrodynamic motions are weak. In Lake Tahoe, such pumping could affect the dispersion of groundwater nutrient inputs, believed to impact nuisance periphyton growth. Though we observed only small amplitude lake-level oscillations, resonant forcing conditions, such as strong atmospheric fronts (Bubalo et al. 2018) or earthquakes (Ichinose et al. 2000), could lead to periods of amplified seiching, causing seiche-related pore-water flow and water quality fluxes to take on additional importance. A seismic fault runs through Lake Tahoe. The seiche structures described here would likely dominate lake hydrodynamics and transport of water quality constituents in the event of a large earthquake.

Main-basin seiche oscillations are present in adjoining water bodies (marinas, wetlands, and bays), implying the existence of seiche-driven exchange flow. Even at small amplitudes, these oscillations can be a dominant driver of flow across the boundaries of these peripheral water bodies, as shown for Emerald Bay. For the case of adjoining wetlands, seiche-driven oscillations were observable hundreds of meters from the approximate lake boundary. During times of low stream flow, the motions driven by such oscillations may represent some of the largest fluxes of material into and out of the wetlands, and should therefore be considered in calculations of net fluxes.

A basic understanding of the presence, spatial patterns, and amplitudes of surface seiches is essential for a complete understanding of the hydrodynamic motions in lakes. In addition to their potential relevance to various in-lake processes, seiche characteristics should be considered in both the siting and the sampling frequencies of instrument deployments. A priori knowledge of nodal patterns can be used to select for processes of interest. When seiches are not of interest to a particular study, their known frequencies can be filtered out to reduce extraneous "noise". If the seiches frequencies are identified ahead of time, sampling frequencies can be set high enough to avoid data aliasing due to under-resolving the seiches.

While the simple geometry of Lake Tahoe and the generally low-amplitude of its resonant barotropic oscillations seemingly reduce interest in a study of its surface seiches, these characteristics ultimately serve to underscore the broad relevance of our results to many lakes, including those without multiple sub-basins and/or without regular noteworthy seiche amplitudes.

Acknowledgements This material is based upon work supported by a National Science Foundation Graduate Research Fellowship (NSF Grant #1650042). Any opinions, findings, and conclusions or recommendations expressed in this material are those of the authors and do not necessarily reflect the views of the National Science Foundation. Support for nearshore water quality stations was generously provided by the Lahontan Regional Water Quality Control Board and through the philanthropic support of several Lake Tahoe community homeowners. Brant Allen, Katie Senft, Brandon Berry, and Raph Townsend, of the UC Davis Tahoe Environmental Research Center, provided invaluable field support. All associated with this publication are available through a UC Davis Library DASH repository at https://doi.org/10.25338/B84C75.

References

Basterretxea G, Jordi A, Garcés E, Anglès S, Reñé A (2011) Seiches stimulate transient biogeochemical changes in a microtidal coastal ecosystem. Mar Ecol Prog Ser 423:15–28

Bokil H, Andrews P, Kulkarni JE, Mehta S, Mitra PP (2010) Chronux: a platform for analyzing neural signals. J Neurosci Methods 192(1):146–151

Bubalo M, Janekovi I, Orlic M (2018) Chrystal and Proudman resonances simulated with three numerical models. Ocean Dyn 68(4–5):497–507

Cimatoribus AA, Lemmin U, Bouffard D, Barry DA (2018) Nonlinear dynamics of the nearshore boundary layer of a large lake (Lake Geneva). J Geophys Res Oceans 123(2):1016–1031

Cyr H (2012) Temperature variability in shallow littoral sediments of Lake Opeongo (Canada). Freshw Sci 31(3):895–907

de Vicente I, Cruz-Pizarro L, Rueda FJ (2010) Sediment resuspension in two adjacent shallow coastal lakes: controlling factors and consequences on phosphate dynamics. Aquat Sci 72(1):21–31

Eiswerth M, Donaldson S, Johnson W (2000) Potential environmental impacts and economic damages of *Eurasian watermilfoil* (*Myriophyllum spicatum*) in western Nevada and northeastern California. Weed Technol 14(3):511–518

Emery WJ, Thomson RE (2001) Time-series analysis methods. In: Emery WJ, Thomson RE (eds) Data analysis methods in physical oceanography, 3rd edn. Elsevier, Amsterdam, pp 371–567

Evans RD (1994) Empirical evidence of the importance of sediment resuspension in lakes. Hydrobiologia 284(1):5–12

Forel FA (1893) Die Schwankungen des Bodensees. Schr Verein Gesch Bodensees 22:49–77

Gardner JV, Mayer LA, Hughs Clarke JE (2000) Morphology and processes in Lake Tahoe (California–Nevada). Bull Geol Soc Am 112(5):736–746

Hamblin PF (1982) On the free surface oscillations of Lake Ontario. Limnol Oceanogr 27(6):1039–1049

Hamblin PF (1998) Exchange flows in lakes. In Imberger J (ed) Physical processes in lakes and oceans, coastal estuarine studies, vol 54. American Geophysical Union, pp 187–198

Hollan E, Rao DB, Bäuerle E (1980) Free surface oscillations in Lake Constance with an interpretation of the "Wonder of the Rising Water" at Konstanz in 1549. Archiv Für Meteorologie Geophysik Und Bioklimatologie Serie A 29(3):301–325

Hutter K, Raggio G, Bucher C, Salvadè G, Zamboni F (1982) The surface seiches of Lake of Lugano. Schweiz Z Hydrol 44(2):455–484

Ichinose GA, Anderson JG, Satake K, Schweickert RA, Lahren MM (2000) The potential hazard from tsunami and seiche waves generated by large earthquakes within Lake Tahoe, California–Nevada. Geophys Res Lett 27(8):1203–1206

Janssen F, Faerber P, Huettel M, Meyer V, Witte U (2005) Pore-water advection and solute fluxes in permeable marine sediments (I):

calibration and performance of the novel benthic chamber system Sandy. Limnol Oceanogr 50(3):768–778
Kirillin G, Engelhardt C, Golosov S (2009) Transient convection in upper lake sediments produced by internal seiching. Geophys Res Lett 36(18):1–5
Kirillin G, Lorang MS, Lippmann TC, Gotschalk CC, Schimmelpfennig S (2015) Surface seiches in Flathead Lake. Hydrol Earth Syst Sci 19(6):2605–2615
Korgen BJ (1995) Seiches. Am Sci 83(4):330–341 **(JSTOR)**
Loeb SL, Goldman CR (1979) Water and nutrient transport via groundwater from Ward Valley into Lake Tahoe. Limnol Oceanogr 24(6):1146–1154
Moore JG, Schweickert RA, Robinson JE, Lahren MM, Kitts CA (2006) Tsunami-generated boulder ridges in Lake Tahoe, California–Nevada. Geology 34(11):965–968
Moore JG, Schweickert RA, Kitts CA (2014) Tsunami-generated sediment wave channels at Lake Tahoe, California–Nevada, USA. Geosphere 10(4):757–768
Mortimer CH, Fee EJ (1976) Free surface oscillations and tides of lakes Michigan and Superior. Philos Trans R Soc A Math Phys Eng Sci 281(1299):1–61
Naranjo RC, Niswonger RG, Smith D, Rosenberry D, Chandra S (2019) Linkages between hydrology and seasonal variations of nutrients and periphyton in a large oligotrophic subalpine lake. J Hydrol 568:877–890
Okamoto I, Endoh S (1995) Water mass exchange between the Main Basin and Shiozu Bay. In: Okuda S, Imberger J, Kumagai M (eds) Physical processes in a Large Lake: Lake Biwa, Japan, vol 48. Coastal and estuarine studies. American Geophysical Union, Washington, DC, pp 31–42
Oldham CE, Lavery PS (1999) Porewater nutrient fluxes in a shallow fetch-limited estuary. Mar Ecol Prog Ser 183:39–47
Precht E, Huettel M (2003) Advective pore-water exchange driven by surface gravity waves and its ecological implications. Limnol Oceanogr 48(4):1674–1684
Rabinovich AB (2009) Seiches and harbor oscillations. In: Kim YC (ed) Handbook of coastal and ocean engineering. World Scientific, Singapore, pp 193–236
Rao DB, Schwab DJ (1976) Two dimensional normal modes in arbitrary enclosed basins on a rotating earth: application to Lakes Ontario and Superior. Philos Trans R Soc A Math Phys Eng Sci 281(1299):63–96
Rao DB, Mortimer CH, Schwab DJ (1976) Surface normal modes of Lake Michigan: calculations compared with spectra of observed water level fluctuations. J Phys Oceanogr 6:575–588
Rueda FJ, Schladow SG (2002) Surface seiches in lakes of complex geometry. Limnol Oceanogr 47(3):906–910
Saylor JH, Miller GS (1987) Studies of large-scale currents in Lake Erie, 1979–80. J Great Lakes Res 13(4):487–514
Saylor JH, Sloss PW (1976) Water volume transport and oscillatory current flow through the straits of Mackinac. J Phys Oceanogr 6(2):229–237
Schwab DJ, Rao DB (1977) Gravitational oscillations of Lake Huron, Saginaw Bay, Georgian Bay, and the North Channel. J Geophys Res 82(15):2105
Sprague HM (2017) Identifying effects of basin-scale waves on hypolimnetic dissolved oxygen : a coherence analysis. University of California, Davis. https://search.library.ucdavis.edu/. Accessed 1 June 2018
van Vugt MK, Sederberg PB, Kahana MJ (2007) Comparison of spectral analysis methods for characterizing brain oscillations. J Neurosci Methods 162(1–2):49–63
Wilson BW (1972) Seiches. In: Chow VT (ed) Advances in hydrosciences, vol 8. Academic Press, Cambridge, pp 1–94
Wittmann ME, Chandra S, Reuter JE, Schladow SG, Allen BC, Webb KJ (2012) The Control ofan Invasive Bivalve, Corbicula fluminea, Using Gas Impermeable Benthic Barriers in a Large Natural Lake. Environmental Management 49(6):1163–1173